Iterative Matrix Fitting Approach of Frequency Dependent Matrices based on Vector Fitting

E.S. Bañuelos-Cabral, J.A. Gutiérrez-Robles, J.J. Nuño-Ayón, M.G. Vega-Grijalva,
J.L. Naredo and J. Sotelo-Castañón.

***Abstract*-- Rational fitting techniques are the basis for modeling the physical behaviors of systems with respect to their input and output characteristics. Due to its robustness and accuracy, Vector Fitting (VF) has been widely used to obtain rational models from tabulated frequency domain responses. Three types of systems could be approximated: 1) A scalar function or scalar fitting (SF) case, 2) A column vector function or column fitting (CF) case, and 3) A matrix function or matrix fitting (MF) case. A common set of poles is desired for physical and implementation reasons. This is a fact in the SF case, and the mathematical formulation of VF allows obtaining a rational function-based model with a common set of poles in the CF case. However, as this is not possible in the MF case, a methodology based on the VF iteration is proposed, which ensures a common set of poles. The advantages are demonstrated in three test cases: 1) Multi-phase transmission-line modeling using the Universal Line Model (ULM), 2) Multi-block data analysis, and 3) Printed Circuit Board (PCB) transmission-line characterization.**

***Keywords*: Frequency-dependent matrices, Multi-block data analysis, PCB transmission-line modeling, Rational approximation, Universal Line Model, Vector Fitting.**

I. Introduction

State-space models are useful for various reasons, such as providing mathematical models that can describe linear as well as nonlinear systems. Furthermore, they can handle not only Single-Input Single-Output (SISO) systems but also Multiple-Input Multiple-Output (MIMO) systems. Indeed, state equations are particularly suited for analyzing and synthesizing MIMO systems [1, 2]. In this context, the search for models that faithfully reproduce the system's behavior with respect to its input and output characteristics is crucial [3]. Vector fitting (VF) is a robust macromodeling method to derive these desired rational function-based models from tabulated frequency domain responses [4]. Different processes have been proposed to obtain these rational approximations of frequency dependent Matrices $(\breve{\boldsymbol{H}}_k)$ through VF using a common set of poles (p_n).

Gustavsen and Semlyen [5, 6] proposed a Matrix Fitting (MF) procedure in 2002 and 2004 for admittance matrices consisting of stacking matrix elements into a single column.

E.S. Bañuelos-Cabral, J.A. Gutiérrez-Robles, J. J. Nuño-Ayón and J. Sotelo-Castañón are with the University of Guadalajara, Mexico.
M.G. Vega-Grijalva is with Intel Corporation, Guadalajara, Mexico.
J.L. Naredo is with Cinvestav-Guadalajara, Guadalajara, Mexico.
(e-mail of corresponding author: eduardo.banuelos@academicos.udg.mx).

Paper submitted to the International Conference on Power Systems Transients (IPST2025) in Guadalajara, Mexico, June 8-12, 2025.

This method allows obtaining common poles for the entire system. However, depending on the matrix size, the resulting column vector can become too large.

In 2008, Gustavsen and Nordstrom [7] presented an improvement to the Universal Line Model based on trace fitting. This process allows obtaining the rational approximation of the characteristic impedance matrix and the propagation function matrices using common poles.

More recently, Macmillan et al. [8] (2024) proposed fitting each column vector using VF, followed by an empirical process to compact poles within a defined area. However, this proposal risks erroneous results if poles overlap.

The aim of this paper is to present an iterative matrix fitting (IMF) approach as an alternative methodology for obtaining rational function-based models using common poles for frequency-dependent matrices based on the VF iteration.

The proposed procedure is demonstrated in (1) Multi-phase transmission-line modeling through the Universal Line Model (ULM), (2) Multi-block data analysis, and (3) PCB transmission-line characterization.

II. Iterative matrix fitting (IMF) approach based on the Vector Fitting iteration

The proposed IMF approach for the rational approximation of frequency-dependent matrices is based on the iterative nature of VF. This iterative process allows creating rational function-based models of frequency-dependent matrices that are not necessarily square, among other advantages.

Let us begin by considering the case for the rational approximation of a scalar function or scalar fitting (SF) case. The goal of VF is to obtain an approximation of a data set through a rational function model in pole-residue form (1) considering a finite number of poles *N*, which are typically defined by the user [4]. These data points can be measured or calculated from some frequency-domain samples: $(s_k, \breve{h}_k)$ where $\breve{h}_k = \breve{h}(s_k)$ for $s_k = \mathrm{j}\omega_k,\ k = 1, \dots, K$.

$$\breve{h}_k \cong h(s;\mathbf{x}) = \sum_{n=1}^{N} \frac{r_n}{s - p_n} + r_0. \tag{1}$$

In (1), $\mathbf{x}$ represents a vector with poles, residues, and the constant term (p_n, r_n, r_0) for the rational approximation.

VF generates this rational function-based model $h(s;\mathbf{x})$ in pole-residue form by relocating a set of initial poles $\{q_n^1 \in \mathbb{C}, n = 1, \dots, N\}$ through an iterative process in a least-squares (LS) sense.

VF works in two stages: First, it iteratively refines the position of the initial poles, (q_n^v), where the number of iterations $(v = 1, \dots, V)$ is also typically defined by the user. Second, it calculates the residues (r_n) and the constant term (r_0) in a single step. This procedure has proven suitable for a Single-Input Single-Output (SISO) state-space modeling [2].

In the LS formulation of VF, solved at each iteration (v), multiple (M) scalar functions $\check{h}_i(s_k), i = 1, \dots, M$ can be considered. As long as they share the same poles, these responses can be stacked in a column vector as: $\check{\mathbf{h}}_k \in \mathbb{C}^M$. This leads to the rational approximation case of a column vector function or column fitting (CF) case. Using this formulation in VF, a set of common poles (2) for this column vector can be obtained: $\left(s_k, \check{\mathbf{h}}_k\right)$ for $k = 1, \dots, K$.

$$\check{\mathbf{h}}_k \cong \mathbf{h}(s; \mathbf{x}) = \sum_{n=1}^{N} \frac{\mathbf{r}_n}{s - p_n} + \mathbf{r}_0. \tag{2}$$

In (2) N common poles (p_n) are used with $\mathbf{r}_n \in \mathbb{C}^M$ for $n = 1, \dots, N$ and $\mathbf{r}_0 \in \mathbb{R}^M$. This formulation is suitable for Single-Input Multiple-Output (SIMO) state-space modeling [2]. According to Gustavsen and Semlyen in [2, 4], this feature gave the method its name: Vector Fitting. Tables I and II show extracts of the VF algorithm for the two aforementioned cases.

TABLE I
VF ALGORITHM FOR SCALAR FITTING (SF)

Input: $\left\{\left(s_k, \check{h}_k\right)\right\}_{k=1}^{K}$ and $\{q_n^1\}_{n=1}^{N}$;
1: **for** $v = 1, \dots, V$ **do**
2: pole relocation, q_n^v, using $\check{h}_k$;
3: **end for**
4: set $p_n = q_n^V$;
5: compute r_n and r_0;
Output: model $h(s; \mathbf{x})$

TABLE II
VF ALGORITHM FOR COLUMN FITTING (CF)

Input: $\left\{\left(s_k, \check{\mathbf{h}}_k\right)\right\}_{k=1}^{K}$ and $\{q_n^1\}_{n=1}^{N}$;
1: **for** $v = 1, \dots, V$ **do**
2: pole relocation, q_n^v, using $\check{\mathbf{h}}_k$;
3: **end for**
4: set $p_n = q_n^V$;
5: compute $\mathbf{r}_n$ and $\mathbf{r}_0$;
Output: model $\mathbf{h}(s; \mathbf{x})$

However, in most cases, it is necessary to model Multiple-Input Multiple-Output (MIMO) systems. Then, we can consider multiple (P) vector functions $\check{\mathbf{h}}_i(s_k), i = 1, \dots P$ collected in a matrix as,

$$\check{\mathbf{H}}_k = \left(\check{\mathbf{h}}_1(s_k), \check{\mathbf{h}}_2(s_k), \dots, \check{\mathbf{h}}_P(s_k)\right). \tag{3}$$

We have now the rational approximation of a matrix function or matrix fitting (MF) case. The challenge here is to find a set of common poles for approximating (4) this matrix function:$\left(s_k, \check{\mathbf{H}}_k\right)$ for $k = 1, \dots, K$, where $\check{\mathbf{H}}_k \in \mathbb{C}^{M \times P}$. In (3) differing numbers of columns and rows are considered.

$$\check{\mathbf{H}}_k \cong \mathbf{H}(s; \mathbf{x}) = \sum_{n=1}^{N} \frac{\mathbf{R}_n}{s - p_n} + \mathbf{R}_0. \tag{4}$$

This case is considered N common poles (p_n) with $\mathbf{R}_n \in \mathbb{C}^{M \times P}$ for $n = 1, \dots, N$ and $\mathbf{R}_0 \in \mathbb{R}^{M \times P}$. Now (4) is suitable for Multiple-Input Multiple-Output (MIMO) state-space modeling [2].

VF's most important feature is arguably its robustness in repositioning initial poles iteratively. Based on this characteristic, we propose an iterative matrix fitting (IMF) approach consisting of using each column vector $(\check{\mathbf{h}}_k \in \mathbb{C}^M)$ for each VF iteration (v). In this way, matrices that are not necessarily square or immittance matrices where the diagonal represents the greatest weight in the array, can be fitted through common poles.

Table III provides an extract of the VF algorithm for the proposed IMF approach which can be directly used with the available VF algorithm. It can be summarized as follows:

Input: The matrix to be fitted, the frequency vector and the initial poles $(\check{\mathbf{H}}_k,\ s_k,\ q_n^1)$.

1: The counter (c) allows the algorithm to iterate through the columns of the matrix a predefined number of times, (V).

2: The poles are repositioned using one column at a time.

9: The set of common poles is obtained $(p_n = q_n^V)$ when the number of iterations (V) is reached.

10: The matrix of residues $(\mathbf{R})$ can be calculated and,

Output: The model is obtained, $\mathbf{H}(s; \mathbf{x})$.

TABLE III
VF ALGORITHM FOR ITERATIVE MATRIX FITTING (IMF) APPROACH

Input: $\left\{\left(s_k, \check{\mathbf{H}}_k\right)\right\}_{k=1}^{K}$ and $\{\{q_n^1\}_{n=1}^{N}$;
1: $c = 1$; (counter)
2: **for** $v = 1, \dots, V$ **do**
3: pole relocation, q_n^v, using $\check{\mathbf{h}}_c(s_k)$;
4: $c = c + 1$;
5: **if** $c == P + 1$ **then**;
6: $c = 1$;
7: **end if**
8: **end for**
9: set $p_n = q_n^V$;
10: compute $\mathbf{R}_n$ and $\mathbf{R}_0$;
Output: model $\mathbf{H}(s; \mathbf{x})$

III. TEST CASES

A. Case I: Transmission-line modeling (ULM)

Electromagnetic waves propagating along an *n*-conductor line or cable are modeled in the frequency domain by Telegrapher's Equations (5), where $\mathbf{V}$ and $\mathbf{I}$ are the voltage and the current vectors of length n. $\mathbf{Z} = \mathbf{R} + \mathrm{j}\omega\mathbf{L}$ and $\mathbf{Y} = \mathbf{G} + \mathrm{j}\omega\mathbf{C} \in \mathbb{C}^{n \times n}$.

$$\frac{d^2\mathbf{V}}{dx^2} = \mathbf{ZYV}, \qquad \frac{d^2\mathbf{I}}{dx^2} = \mathbf{YZI}. \tag{5}$$

At the ends $x = 0$ and $x = L$ of the line, the following equations relate incident current waves to those reflected from the opposite end:

$$\mathbf{I}_0 - \mathbf{Y}_c\mathbf{V}_0 = -\mathbf{H}[\mathbf{I}_L + \mathbf{Y}_c\mathbf{V}_L], \tag{6}$$

$$\mathbf{I}_L - \mathbf{Y}_c\mathbf{V}_L = -\mathbf{H}[\mathbf{I}_0 + \mathbf{Y}_c\mathbf{V}_0]. \quad (7)$$

Where $\mathbf{Y}_c = \mathbf{Z}^{-1}\sqrt{\mathbf{ZY}} = \sqrt{(\mathbf{YZ})^{-1}}\mathbf{Y}$ and $\mathbf{H} = e^{-\sqrt{\mathbf{YZ}}l}$ with $\mathbf{Z}$, $\mathbf{Y}$, $\mathbf{Y}_c$, $\mathbf{H}$, and l being the line series impedance per unit length, shunt admittance per unit length, characteristic admittance matrix, propagation function matrix, and length, respectively. The term $\mathbf{Y}_c\mathbf{V}_0$ in (6) can be defined as a shunt current at $x = 0$:

$$\mathbf{I}_{sh,0} = \mathbf{Y}_c\mathbf{V}_0. \quad (8)$$

Moreover, denoting $\mathbf{I}_H$ in (6) as,

$$\mathbf{I}_{H0} = \mathbf{H}[\mathbf{I}_L + \mathbf{Y}_c\mathbf{V}_L] = \mathbf{H}\mathbf{I}_{far,L}. \quad (9)$$

Where $\mathbf{I}_{far}$ is the reflected current wave from the opposite line end, the voltage/current relationship at the ends of a transmission line is established. In the application of the ULM [9, 10] for the multi-conductor examples, the trace fitting (TF) approach is commonly implemented. This concept minimizes CPU time and memory requirements [7]. In accordance with the TF, $\mathbf{Y}_c$ is approximated in the phase domain through,

$$\mathbf{Y}_c \cong \sum_{m=1}^{N_y} \frac{\mathbf{G}_m}{s - p_m} + \mathbf{D}, \quad (10)$$

where $\mathbf{D}$ is a constant matrix, $\mathbf{G}_m$ is a matrix of residues, and N_y is the number of poles. When using modal decomposition for $\mathbf{H}$, it can be written as:

$$\mathbf{H} = \mathbf{T}\mathbf{H}_m\mathbf{T}^{-1}, \quad (11)$$

where $\mathbf{T}$ is the eigenvector matrix and $\mathbf{H}_m$ is a diagonal matrix $\mathbf{H}_m = diag\left[e^{-\lambda_1 l}, e^{-\lambda_2 l}, \ldots, e^{-\lambda_N l}\right]$, with $\lambda = \sqrt{\mathbf{YZ}}$ being the propagation constant of the conductor line.

Idempotent decomposition is applied for the synthesis of $\mathbf{H}$ in the phase domain as follows:

$$\mathbf{H} = \sum_{i=1}^{N_h} \mathbf{\Gamma}_i e^{-\lambda_i l} = \sum_{i=1}^{N_h} \mathbf{\Gamma}_i e^{-\lambda_i{}' l} e^{-s\tau_i} = \sum_{i=1}^{N_h} \widetilde{\mathbf{H}}_i e^{-s\tau_i}, \quad (12)$$

where τ_i represents the time delays and $\mathbf{\Gamma}_i$ is the idempotent square matrix derived from multiplying the i-th column of $\mathbf{T}$ with the i-th row of $\mathbf{T}^{-1}$.

After identifying the time delay for each mode, $\widetilde{\mathbf{H}}_i$ is approximated using the TF approach [7] with a common set of poles. Ultimately, the multi-delayed rational function-based model for $\mathbf{H}$ in the phase domain is,

$$\mathbf{H} \cong \sum_{i=1}^{N_h} \left(\sum_{k=1}^{N_i} \frac{\mathbf{R}_{i,k}}{s - p_{i,k}} \right) e^{-s\tau_i}, \quad (13)$$

where N_h is the number of propagation modes, N_i is the number of poles for the i-th mode, and $\mathbf{R}_{i,k}$ is a matrix of residues.

The test case is then modeled using our own algorithm in MATLAB. The source and the three-phase delta transmission line configuration for the test case are shown in Fig. 1. The line is energized from a balanced three-phase voltage source behind an impedance (L_s). Moreover, 500 log-spaced samples are used for the calculation of $\mathbf{Z}$ and $\mathbf{Y}$, 15 poles for the rational approximation of $\mathbf{Y}_c$, and 30 poles for each $\widetilde{\mathbf{H}}_i$.

Simulation of the transmission line is performed first, using the TF for the rational approximation of $\mathbf{Y}_c$ and $\widetilde{\mathbf{H}}_i$; and then using the IMF approach.

The results of the rational approximations are shown in Figs. 2, 3, 4 and 5, including their calculation of the RMS-errors. Finally, the voltage source (V_s), voltage at sending end (V_0) and voltage at receiving end (V_L) of phase A, using both TF and IMF are shown in Fig. 6 for open line end.

The results are practically identical for both methodologies.

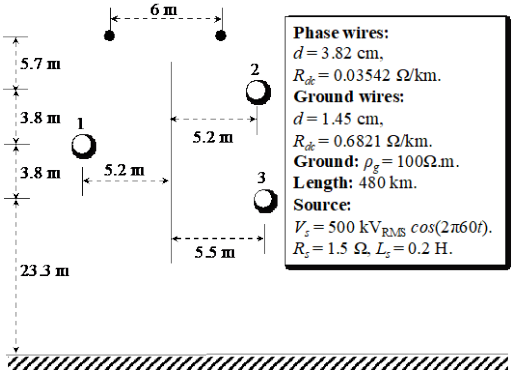

Fig. 1. Three-phase delta transmission line configuration.

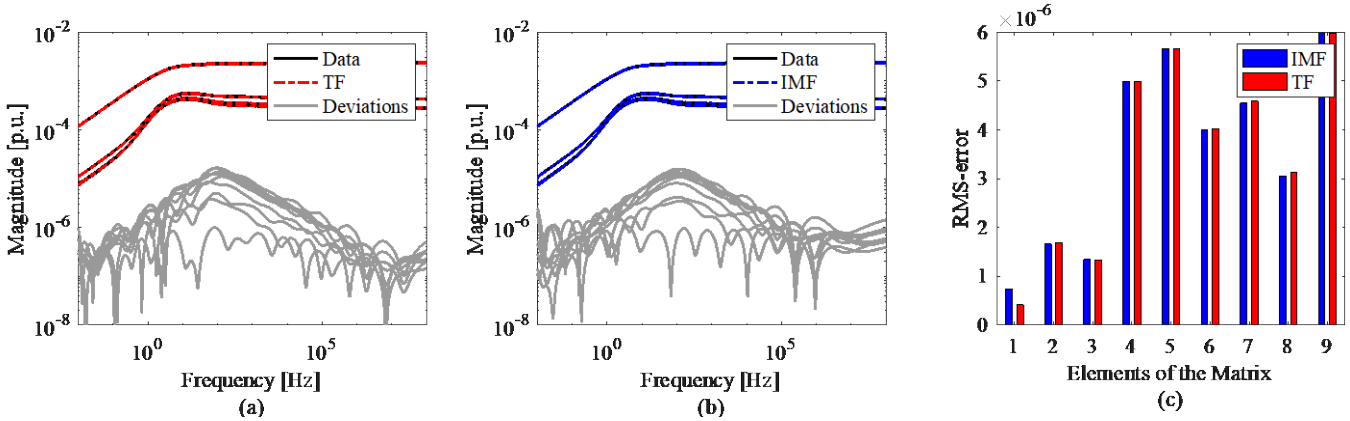

Fig. 2. (a) $\mathbf{Y}_c$ and its approximation using TF, (b) $\mathbf{Y}_c$ and its approximation using IMF, and (c) RMS-error of the rational approximations.

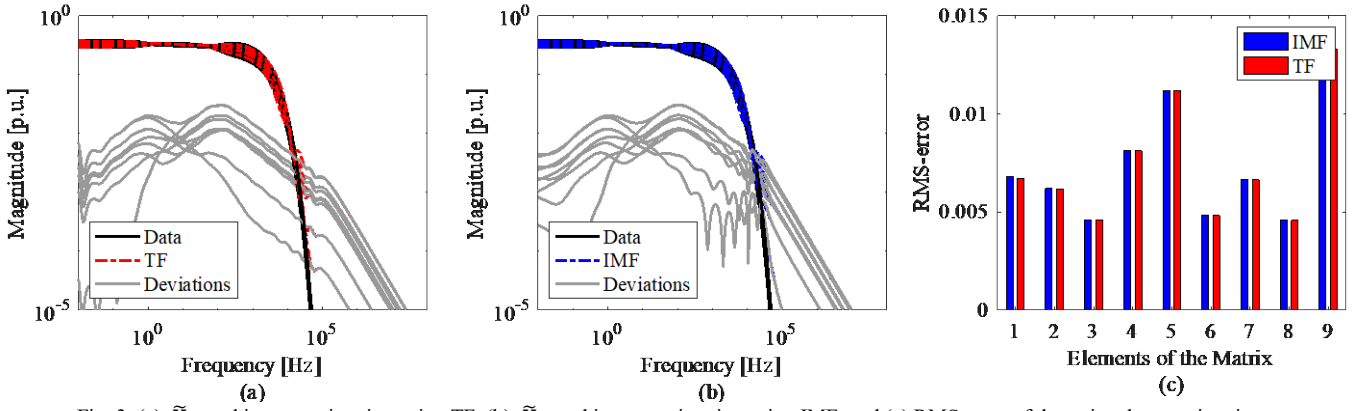

Fig. 3. (a) $\tilde{\mathbf{H}}_1$ and its approximation using TF, (b) $\tilde{\mathbf{H}}_1$ and its approximation using IMF, and (c) RMS-error of the rational approximations.

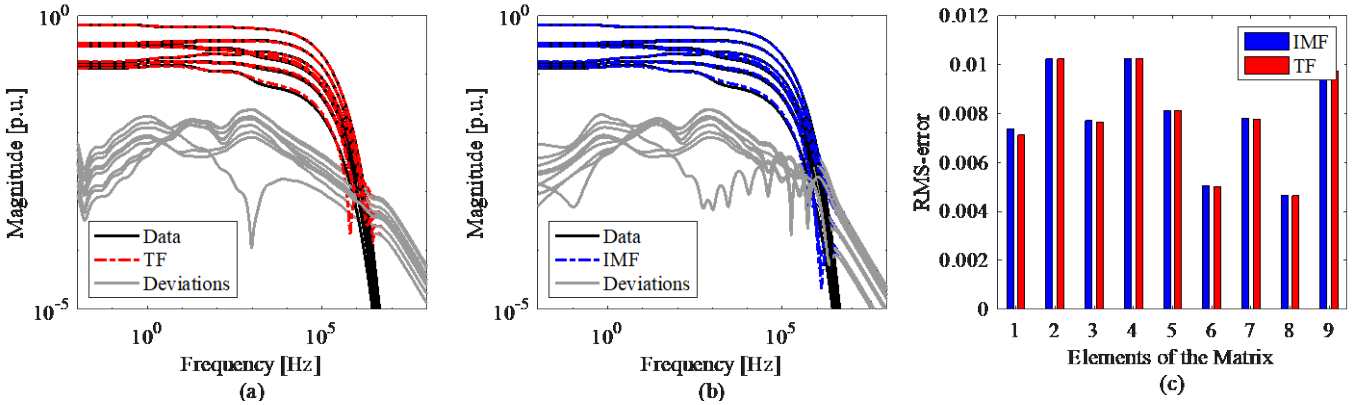

Fig. 4. (a) $\tilde{\mathbf{H}}_2$ and its approximation using TF, (b) $\tilde{\mathbf{H}}_2$ and its approximation using IMF, and (c) RMS-error of the rational approximations.

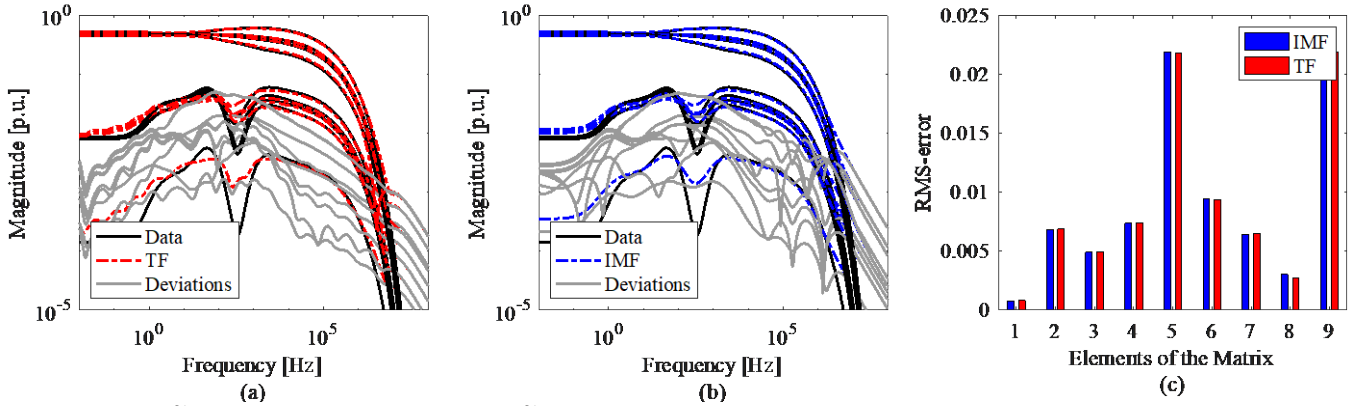

Fig. 5. (a) $\tilde{\mathbf{H}}_3$ and its approximation using TF, (b) $\tilde{\mathbf{H}}_3$ and its approximation using IMF, and (c) RMS-error of the rational approximations.

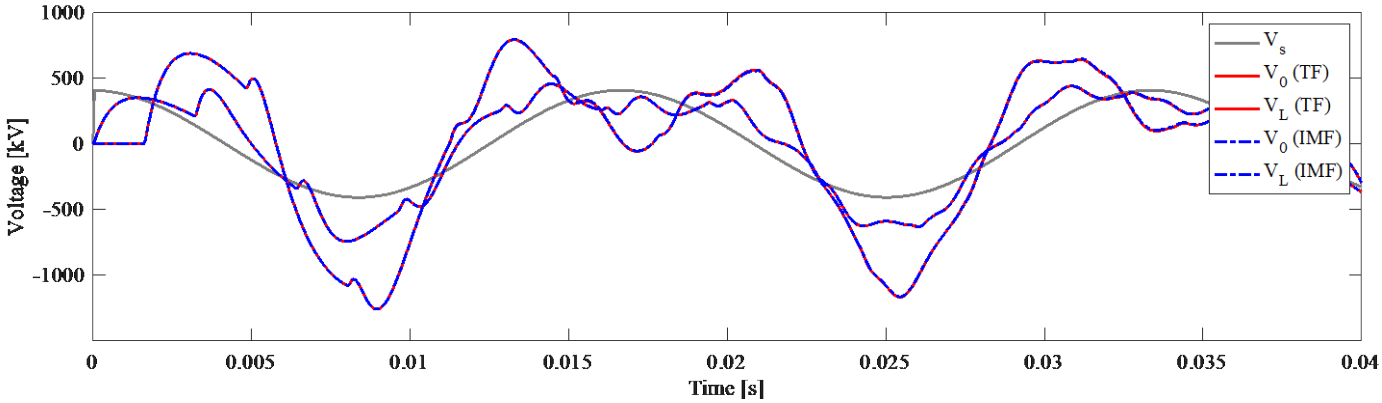

Fig. 6. Voltage source (V_s), voltage at sending end (V_0) and, voltage at receiving end (V_L) of phase A, using both TF and IMF approaches.

B. Case II: Multi-block data analysis

Wide area measurement systems based on phasor measurement units allow recording multiple data such as voltage, frequency, and active or reactive power under transient conditions and have motivated the development of multi-block data analysis techniques [11]. The transient data recorded may reveal electromechanical oscillation modes that should be identified as they provide valuable information about the stability of the electrical system [12].

A measurement of an electrical power system $(f(t))$ containing $N/2$ oscillatory modes can be approximated by,

$$f(t) \cong \varepsilon + \sum_{n=1}^{N/2} a_n e^{\alpha_n t} \cos(\omega_n t + \theta_n). \quad (14)$$

Where ε is a direct component, a_n is the amplitude for the nth mode, α_n is the n-th damping factor, ω_n is the frequency for the n-th mode, and θ_n is the corresponding phase for each mode. It is also possible to consider multiple (M) measurements, as follows [12]:

$$\mathbf{f}(t) \cong \boldsymbol{\varepsilon} + \sum_{n=1}^{N/2} \mathbf{a}_n e^{\alpha_n t} \cos(\omega_n t + \boldsymbol{\theta}_n). \quad (15)$$

Where $\mathbf{f}$ and $\boldsymbol{\varepsilon} \in \mathbb{R}^M$ and $\mathbf{a}_n$ and $\boldsymbol{\theta}_n \in \mathbb{R}^M$ for $n = 1, \dots, N$. Note that common frequencies and dampings have been considered, that is, common poles in the frequency domain (FD). Finally, a multi-block data matrix $\mathbf{F}(\mathrm{t}_k)$ for $k = 1, \dots, K$ can be considered, consisting of (P) column vectors containing (M) measurements, and approximated as follows [12]:

$$\mathbf{F}(t) \cong \mathbf{E} + \sum_{n=1}^{N/2} \mathbf{A}_n e^{\alpha_n t} \cos(\omega_n t + \boldsymbol{\Theta}_n). \quad (16)$$

Where $\mathbf{F}(t)$ and $\mathbf{E} \in \mathbb{R}^{M \times P}$ and $\mathbf{A}_n$ and $\boldsymbol{\Theta}_n \in \mathbb{R}^{M \times P}$ for $n = 1, \dots, N$. Using the Numerical Laplace Transform (NLT) is possible to obtain the image of $\mathbf{F}(t)$ in FD to implement the proposed IMF to estimate oscillatory modes from the multi-block transient data [13]. Clearly (14), (15), and (16) correspond to scalar fitting (SF), column fitting (CF), and matrix fitting (MF), respectively.

To evaluate the proposed IMF, several transient responses are obtained from a simulation of the IEEE 16-generator 5-area power system using the Power System Toolbox (PST); the power system parameters can be found in [12].

Fig. 7 shows a single-line diagram of this system formed by 16 generators, 68 buses, and 86 transmission lines divided into 5 areas. A contingency case is created by introducing a three-phase fault at the end of the transmission line 41-42 and clearing it after 20 ms. The active power signals, reactive power signals, and speed signals from all generators are recorded for 25 seconds with a sampling rate of 100 samples per second. Fig. 8 shows the oscillatory behavior of these signals with their mean values removed. The rational approximations for the images of active power, reactive power, and speed signals in FD are shown in Fig. 9 including the corresponding RMS-error calculations where $N = 10$ poles have been used.

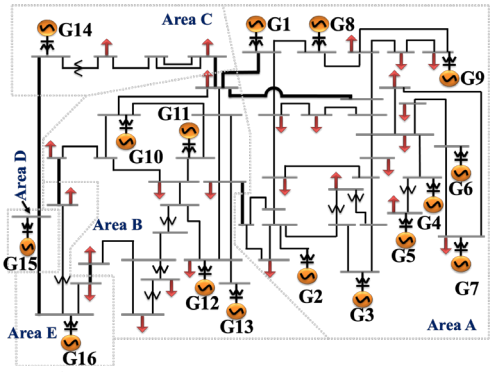

Fig. 7. IEEE 16-generator 5-area power system.

Table IV shows the modal parameter estimation through the IMF approach, based on the multi-block data formed by the active power signals, reactive power signals, and speed signals. As shown, three dominant oscillation modes were identified at 0.2383 Hz, 0.3940 Hz, and 0.6288 Hz. These results confirm that the IMF allows estimating modal parameters from multi-block data. Finally, to validate these results, Koopman Mode Decomposition (KMD) [14] was applied to each group of signals, since the method cannot be applied to multi-block data matrices, $(\mathbf{F}(\mathrm{t}_k))$. As seen in Table V, the KMD method also estimates three dominant inter-area modes, which are consistent with the oscillation modes presented in Table IV for the IMF.

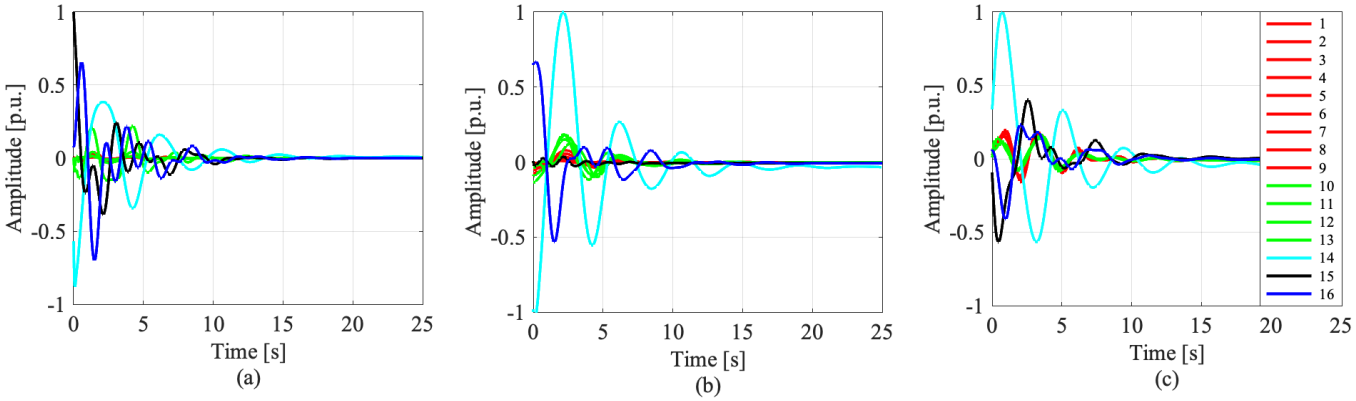

Fig. 8. (a) Active power signals, (b) Reactive power signals, (c) Speed signals.

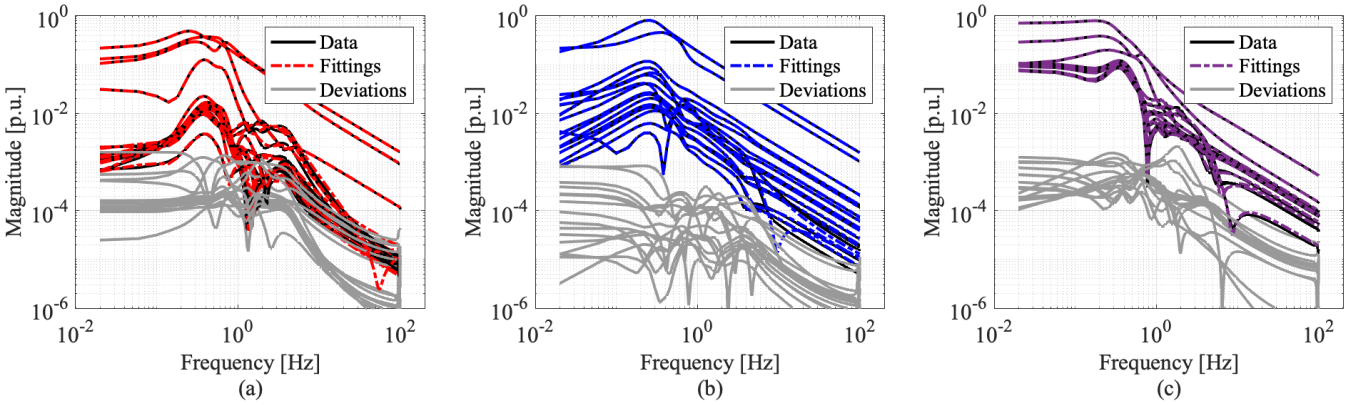

Fig. 9. Images in FD and their approximations for (a) Active power signals, (b) Reactive power signals, and (c) Speed signals.

TABLE IV
MODAL PARAMETER ESTIMATION USING THE IMF APPROACH.

Mode 1		Mode 2		Mode 3	
Frequency [Hz]	Damping	Frequency [Hz]	Damping	Frequency [Hz]	Damping
0.2383	-0.3391	0.3940	-0.2903	0.6288	-0.4046

TABLE V
MODAL PARAMETER ESTIMATION USING THE KMD METHOD.

Mode 1		Mode 2		Mode 3	
Frequency [Hz]	Damping	Frequency [Hz]	Damping	Frequency [Hz]	Damping
0.2308	-0.2653	0.3637	-0.3281	0.6357	-0.3632
0.2339	-0.2723	0.3627	-0.2852	0.6382	-0.3056
0.2336	-0.2881	0.3721	-0.2843	0.6368	-0.3352

C. Case III: PCB transmission-line characterization

This case involves the analysis of a double differential pair PCB transmission-line composed by four-line segments and two vias [15], as shown in Fig. 10.

The test points on the transmission-line are connected at points P and Q with a VNA (model-N5247A) to obtain the S-parameters. The measurement device has been configured with a bandwidth of 10 MHz to 20 GHz and 2000 linearly spaced samples. Given a system: $\widetilde{\mathbf{H}}_k \in \mathbb{C}^{4\times4}$, $k = 1, \ldots, 2000$, the transfer function $(\mathbf{H}(s;\mathbf{x}))$ is then calculated using 350 poles with SF for each matrix element and 350 common poles with TF, IMF and CF.

The results of these rational approximations are shown in Figs. 11a, 11b, 12a and 12b, respectively. The RMS-error according to each iteration can be seen in Fig. 13a for SF and TF and the corresponding RMS-errors for each element of the matrix considering these different approaches are shown in Fig. 13b.

SF obtains the lowest errors but does not employ common poles. IMF shows comparable error rates utilizing common poles and they are even better than CF. TF has the highest error rates of the three methodologies. Following, Fig. 14a shows the poles calculated for each approach.

Finally, in Fig. 14b, the time domain voltage responses of the return loss parameter (S11) are shown for each model obtained using SF, TF, IMF and CF by sending a unit pulse with a duration of 200 ps, a rise time of 50 ps and a delay of 1 ns where the response using the Discrete Fourier Transform (DFT) has been taken as the reference.

The models obtained with SF and TF are the least accurate, followed by the model obtained with CF, and the most accurate is IMF, which practically overlaps the response calculated with the DFT.

It is remarkable that CF uses all columns in each iteration while IMF uses only 25% of the data corresponding to one column, and although it uses less data it is more accurate. These results validate the IMF approach proposed in this work.

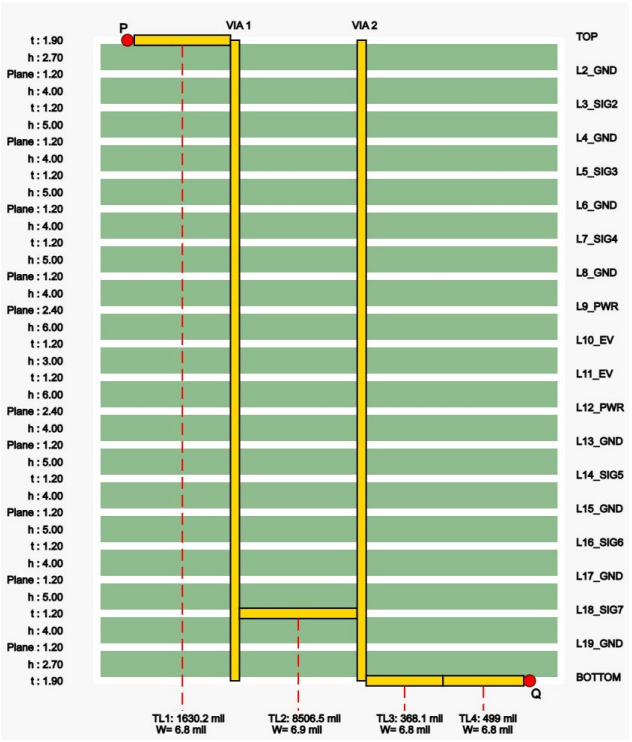

Fig. 10. PCB cross section.

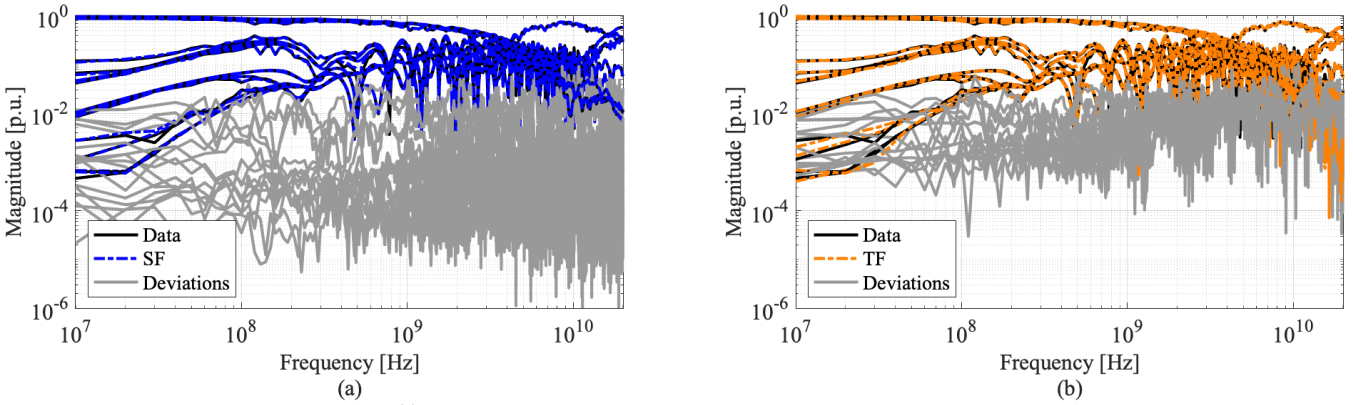

Fig. 11. $\breve{\mathbf{H}}_k$ and its approximation with, (a) the SF approach and (b) TF approach.

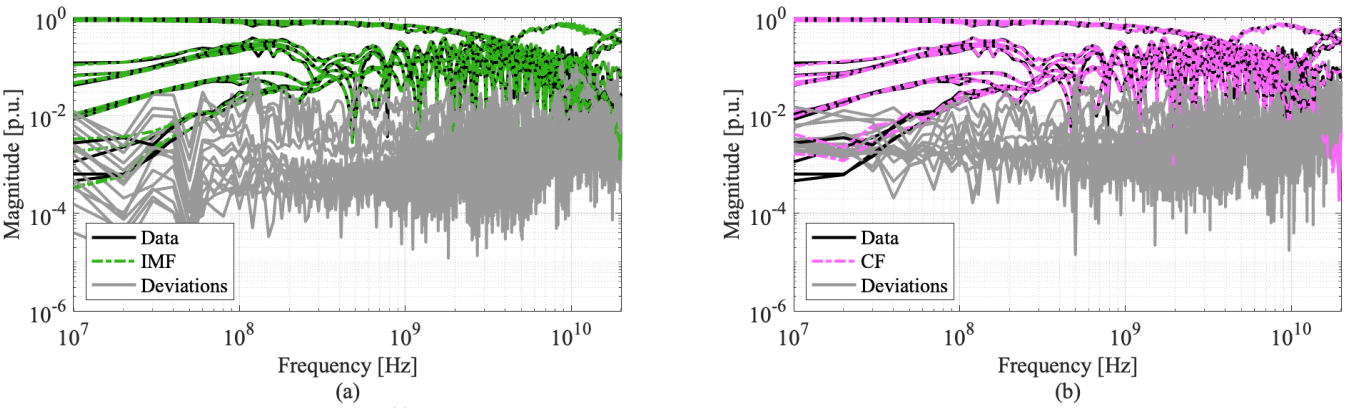

Fig. 12. $\breve{\mathbf{H}}_k$ and its approximation with, (a) the IMF approach and (b) CF approach.

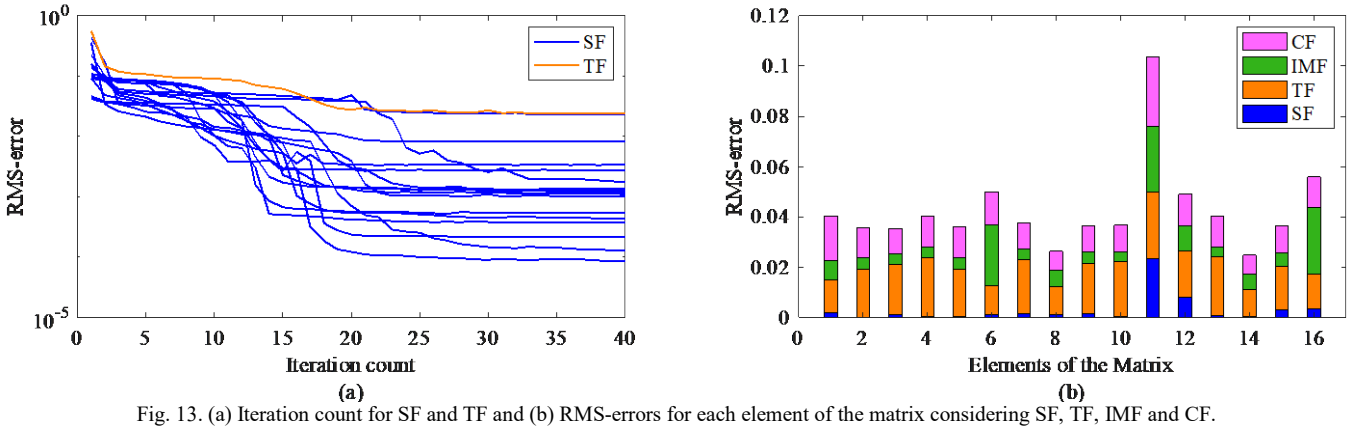

Fig. 13. (a) Iteration count for SF and TF and (b) RMS-errors for each element of the matrix considering SF, TF, IMF and CF.

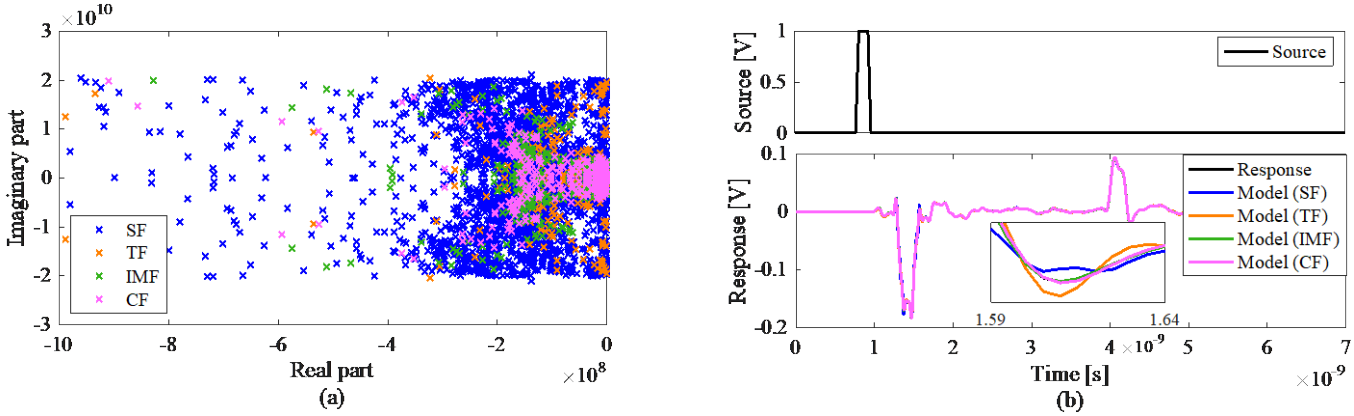

Fig. 14. (a) Calculated poles considering SF, TF, IMF and CF, (b) Time domain responses using SF, TF, IMF and CF approaches.

IV. Conclusions

An iterative matrix fitting (IMF) approach has been introduced as an alternative methodology to obtain rational function-based models using common poles of frequency-dependent matrices, building on the VF iteration. The proposed methodology was applied in multi-phase transmission-line modeling, data analysis from a multi-block matrix, and PCB transmission-line characterization.

The main findings are as follows:

1) When a system shares common poles, it may seem a practical solution to approximate a matrix $(\check{\mathbf{H}}_k)$ using the common poles calculated from one of their column vectors $(\check{\mathbf{h}}_k)$. However, challenges can arise, particularly in admittance matrices, where the diagonal elements carry the majority of the matrix's weight. In such a case, the TF methodology may be a solution. However, the IMF approach has proven to be a better option.

2) In the test case of multi-phase transmission-line modeling through the Universal Line Model (ULM); the results indicate that the trace fitting (TF) process and the proposed IMF methodology offer practically the same error levels.

3) The combination of the Numerical Laplace Transform (NLT) with the VF method is a powerful tool for multi-block data analysis, particularly in systems based on phasor measurement units. These systems may involve non-square matrices and large number of measured signals, which prevents stacking the matrix elements into a single column vector. The proposed methodology overcomes this limitation and allows identifying the desired parameters.

4) In the case of PCB transmission-line characterization, the IMF approach shows better results compared to the approximation using the TF and CF methodologies.

5) Rational function-based models are required to comply with some important properties as passivity. This property has commonly been forced to be fulfilled at a post-processing stage. Compliance with the model passivity may be assessed and enforced for all methodologies presented (SF, TF, IMF and CF).

6) According to the presented test cases, it is highlighted that IMF methodology uses less data in comparison with CF and its precision may be equal or better.

V. References

[1] C.P. Lathi, Linear Systems and Signals, 2nd ed., Oxford University Press, New York, 978-0195158335, 2005.

[2] S. Grivet-Talocia and B. Gustavsen, Passive Macromodeling. Theory and applications, John Wiley & Sons, Inc. 978-1118094914, 2015.

[3] A. Ramirez and B. Gustavsen, "Relaxed Nonlinear Vector Fitting for Calculation of Rational Approximation of Systems Defined by Input/Output Responses in the Frequency Domain," *IEEE Transactions on Power Delivery*, vol. 39, no. 5, pp. 2965-2972, Oct. 2024.

[4] B. Gustavsen and A. Semlyen, "Rational approximation of frequency domain responses by vector fitting," *IEEE Transactions on Power Delivery*, vol. 14, no. 3, pp. 1052-1061, July 1999.

[5] B. Gustavsen, "Computer code for rational approximation of frequency dependent admittance matrices," *IEEE Transactions on Power Delivery*, vol. 17, no. 4, pp. 1093-1098, Oct. 2002.

[6] B. Gustavsen and A. Semlyen, "A robust approach for system identification in the frequency domain," *IEEE Transactions on Power Delivery*, vol. 19, no. 3, pp. 1167-1173, July 2004.

[7] B. Gustavsen and J. Nordstrom, "Pole Identification for The Universal Line Model Based on Trace Fitting," *IEEE Transactions on Power Delivery*, vol. 23, no. 1, pp. 472-479, Jan. 2008.

[8] A. M. Smith, S. D'Arco, J. A. Suul and B. Gustavsen, "Improved Pole Placement and Compaction of MIMO Vector Fitting Applied to System Identification," *IEEE Transactions on Power Delivery*, vol. 39, no. 2, pp. 1259-1270, April 2024.

[9] A. Morched, B. Gustavsen and M. Tartibi, "A universal model for accurate calculation of electromagnetic transients on overhead lines and underground cables," I*EEE Transactions on Power Delivery*, vol. 14, no. 3, pp. 1032-1038, July 1999.

[10] E.S. Bañuelos-Cabral, B. Gustavsen, J.A. Gutiérrez-Robles, H.K. Høidalen, J.L. Naredo, "Computational efficiency improvement of the Universal Line Model by use of rational approximations with real poles," *Electric Power Systems Research*, vol. 140, pp. 424-434, 2016.

[11] A. Román-Messina, A. Castillo-Tapia, D. A. Román-García, M. A. Hernández-Ortega, C. A. Morales-Rergis and C. M. Castro-Arvizu, "Distributed Monitoring of Power System Oscillations Using Multiblock Principal Component Analysis and Higher-order Singular Value Decomposition," *Journal of Modern Power Systems and Clean Energy*, vol. 10, no. 4, pp. 818-828, July 2022.

[12] G. Rogers, Power System Oscillations, Norwell, Kluwer, 2000.

[13] E.S. Bañuelos-Cabral, J.J. Nuño-Ayón, B. Gustavsen, J.A. Gutiérrez-Robles, V.A. Galván-Sánchez, J. Sotelo-Castañón, J.L. García-Sánchez, "Spectral fitting approach to estimate electromechanical oscillation modes and mode shapes by using vector fitting," *Electric Power Systems Research*, vol. 176, 2019.

[14] Marcos Alfredo Hernández Ortega and Arturo Román Messina, "An Observability-based Approach to Extract Spatiotemporal Patterns from Power System Koopman Mode Analysis, " *Electric Power Components and Systems*, vol. 45, no. 4, pp. 355-365. 2017.

[15] R. Achar and M. S. Nakhla, "Simulation of high-speed interconnects," *Proceedings of the IEEE*, vol. 89, no. 5, pp. 693-728, May 2001.